G. Zhang, H. Rahbardar Mojaver, A. Das, and O. Liboiron-Ladouceur, "Mode insensitive switch for on-chip interconnect mode division multiplexing systems," Optics Letters, vol. 45, no. 4, pp. 811-814, 2020.

https://www.osapublishing.org/ol/abstract.cfm?uri=ol-45-4-811

Optics Letters

Mode insensitive switch for on-chip interconnect mode division multiplexing systems

Guowu Zhang,* Hassan Rahbardar Mojaver, Alok Das, and Odile Liboiron-Ladouceur

Department of Electrical and Computer Engineering, McGill University, Montreal, Quebec H3A 0E9, Canada
**Corresponding author: guowu.zhang@mail.mcgill.ca*

Received 3 December 2019; revised 26 December 2019; accepted 30 December 2019; posted 8 January 2020 (Doc. ID 384771); published 6 February 2020

A mode insensitive switch is proposed and experimentally demonstrated on a silicon-on-insulator platform using a balanced Mach–Zehnder interferometer structure with a mode insensitive phase shifter for on-chip mode division multiplexing interconnects. Switching the first three quasi-transverse electric (TE) modes, consuming less than 40 mW power is demonstrated. The whole system exhibits approximately −2, −3.7, and −5.2 dB insertion loss for the TE0, TE1, and TE2 modes at 1550 nm, respectively. The corresponding crosstalk is less than −8.6 (−9), −8(−10.3), and −10 dB (−10.3 dB) within the wavelength range of 40 nm (1535–1575 nm) for the cross (bar) states, respectively. The extinction ratios (ERs) for the cross (bar) states are 20.1 (19.5), 22.8 (33.7), and 15.4 dB (18.1 dB) for the TE0, TE1, and TE2 modes at 1550 nm, respectively. The payload transmission is also conducted using non-return-to-zero pseudorandom binary sequence (PRBS)-31 data signals at 10 Gb/s for single-mode transmission and simultaneous three-mode transmissions. For all the scenarios, open eyes are observed.

https://doi.org/10.1364/OL.384771

Silicon photonics has been investigated intensively in the past decades due to its several appealing features, such as low absorption coefficients within a large wavelength range, high-index contrast between the silicon waveguide core and the surrounding oxide, and compatibility with the existing fabrication technology for complementary metal-oxide-semiconductor technology [1]. To further increase the data transmission capacity, multiplexing techniques are often employed, such as polarization division multiplexing, wavelength division multiplexing (WDM), and mode division multiplexing (MDM). Among all these techniques, MDM is of great interest, since it utilizes one laser source to modulate all channels. This helps reduce the power consumption compared with other multiplexing techniques [2]. Several key components are required for realizing an on-chip MDM system, such as a mode demultiplexer (deMUX) [3], multimode waveguide bend [4,5], multimode crossing [6], multimode 3 dB splitter [7], higher-order mode filter [8], and multimode switch [9–12]. Among these, the multimode switch is of great importance, since it makes MDM systems more flexible by switching between different channels.

Several MDM switches have been previously proposed. In Refs. [9,10], WDM-compatible MDM switch is proposed and demonstrated using microring resonators. Using symmetric Y junctions and multimode interference (MMI) couplers, we demonstrated a high-speed mode switch for switching between two modes using a PN junction-based phase shifter [11]. Based on a densely packed waveguide array, a two-mode switch is also demonstrated [12]. MDM-compatible matrix switches are also proposed and demonstrated in Ref. [13] which follows a demultiplexing-switching-multiplexing strategy. Recently, we also reported several MDM mode switches using MMI-based structures [14,15] as a mode decomposer and single-mode phase shifter. These switches [14,15] exhibit inter-modal switching operation and are realized using a Mach–Zehnder interferometer MZI) structure where the phase shifter works only for fundamental mode.

In this Letter, we propose and experimentally demonstrate a mode insensitive switch that is capable of switching the first three TE modes simultaneously employing a mode insensitive phase shifter and balanced MZI structures. By taking advantage of the mode insensitive phase shifter, the switch exhibits ultra-low power consumption, since all the modes share the same phase shifter. A balanced MZI structure is employed in this design considering its broadband response. The switch was fabricated by Applied Nanotools Inc. (ANT) and characterized in our lab. The experimental results show that the fabricated mode insensitive switch can switch three modes with an extinction ratio (ER) of 20.1 (19.5), 22.8 (33.7), and 15.4 dB (18.1 dB) for the cross (bar) states while consuming only 38.4 mW power. The payload transmission is conducted from which open eye diagrams can be observed. The proposed switch can be used to connect different modules in an optical interconnect network using MDM, such as data centers.

The proposed device is designed for fabrication on an silicon-on-insulator chip with the optical waveguide thickness of 220 nm. The cross sections of the waveguides for the fundamental mode (TE0), two modes (TE0, TE1), and three modes (TE0, TE1, and TE2) and simulated effective index as a function of the

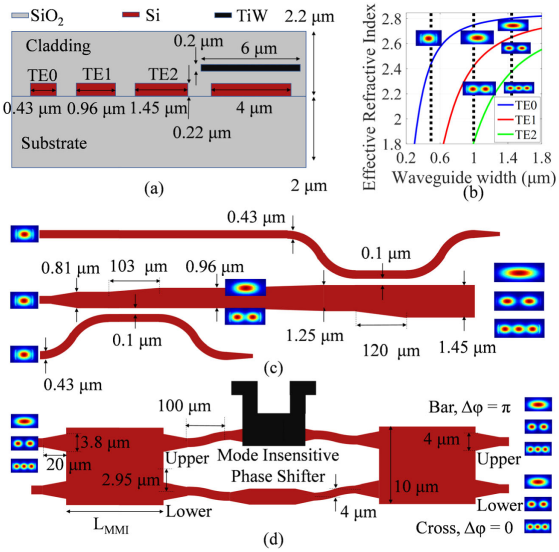

Fig. 1. (a) Cross section of the fundamental mode (TE0), two-mode (TE0, TE1), and three-mode (TE0, TE1, and TE2) waveguides and phase shifter; (b) simulated effective refractive index as a function of waveguide width; (c) schematic of the mode multiplexer and demultiplexer; (d) schematic of the proposed mode insensitive switch.

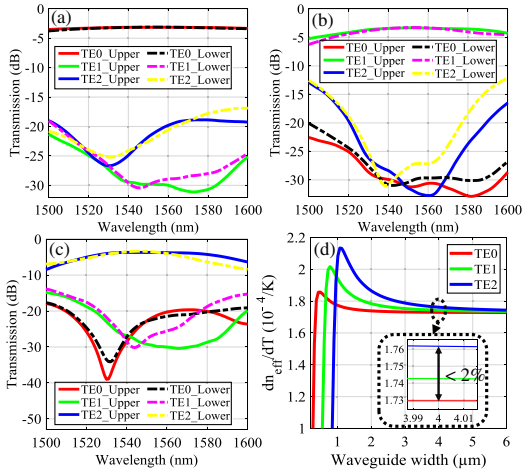

Fig. 2. Simulated transmission spectrum of the multimode MMI for (a) TE0 input, (b) TE1 input, and (c) TE2 input. (d) Simulated dn_{eff}/dT as a function of the phase shifter width for the first three TE modes.

waveguide width are shown in Figs. 1(a) and 1(b). The widths for the fundamental mode (TE0), two-mode (TE0, TE1), and three-mode (TE0, TE1, and TE2) waveguides are selected to be 0.43, 0.96, and 1.45 μm to support the higher-order modes. The input optical beam for TE0, TE1, and TE2 modes are converted into the corresponding modes using an adiabatic coupler-based mode multiplexer [3] because of its large fabrication tolerance. The structure of the mode multiplexer is shown in Fig. 1(c) and the detailed parameters are selected according to the results of our previous study [14]. Specifically, the input, output waveguide width of the bus waveguide and the length of the taper are 0.81 (1.25), 0.96 (1.45), and 103 μm (120 μm) for TE1 (TE2) mode multiplexers, respectively. The output beam of the mode multiplexer is power divided using a well-designed multimode 3 dB coupler based on the MMI. The schematic diagram of the proposed 2 × 2 mode insensitive switch is shown in Fig. 1(d). The outputs of the MMI are separated by multimode S bend to make sure the separation of the two arms of the MZI is large enough so that the thermal crosstalk is lowered enough. To ensure that the multimode S bend has a low crosstalk and as compact as possible, we choose the input radius of the S bend to be 1000 μm to reduce the mode mismatch and the length to be 100 to reduce the footprint of the device. Then a mode insensitive phase shifter is employed to alter the phase of the three different modes simultaneously. After that, another MMI-based 3 dB splitter is used to realize a balanced MZI structure. The output of the switch is demultiplexed using the same structure as in the mode multiplexer part. The schematic of the switch is shown in Fig. 1(d).

To get a good two-fold image of all the three input modes, the multimode MMI width is selected to be 10 μm to support a sufficient mode in the multimode region. The beat length (L_π) is initially calculated using Eq. (1) and further optimized with a commercial software Lumerical:

$$L_\pi = \frac{\pi}{\beta_0 - \beta_1} = \frac{4 n_{\text{eff}} W_m^2}{3\lambda_0}, \tag{1}$$

where β_0 and β_1 are the propagation constants of the first two order TE modes in the multimode region, n_{eff} is the effective index, W_m is the width of the MMI, and λ_0 is the desired wavelength. The MMI is working at the general interference input mode. The length was further optimized using an eigenmode expansion solver; the final optimized length is 362 μm. Figures 2(a)–2(c) show the transmission spectrum of the 3 dB splitter when the three TE modes are fed into the upper input port. The upper and lower ports are defined in Fig. 1(d). The simulated relative phase of two MMI outputs are 90°±0.5°, 90°±2°, and 90°±5° within the wavelength of 1520–1580 nm for TE0, TE1, and TE2, respectively. The crosstalk for TE0 and TE1 is mainly from TE2 input because of the imperfect imaging of the higher-order input. The length of the MMI is long since the width of the MMI is wider to support enough modes. The length of the MMI can be reduced using a subwavelength grating-based MMI where one can engineer the refractive index in the multimode region [16].

To make a mode insensitive switch, a mode insensitive phase shifter is needed. Realizing a mode insensitive phase shifter is challenging since different modes have different propagation constants. However, in the simulation, we found that the change in the rate of the effective index with respect to the local temperature (dn_{eff}/dT) converges toward almost the same value for three different TE modes by increasing the phase shifter width. The design of the mode insensitive phase shifter is accomplished by calculating dn_{eff}/dT for different TE modes using a commercial CAD tool from Lumerical. Figure 2(d) shows the simulated dn_{eff}/dT as a function of the phase shifter width. In particular, when the waveguide width is larger than 4 μm, the difference between the values of the dn_{eff}/dT for the first three TE modes is less than 2% (±1%). However, the heater power consumption increases with the waveguide width. To optimize both power consumption and mode insensitivity, we choose the width of the phase shifters as 4 μm. The experimental results also validate the choice of 4 μm is sufficient for the three-mode switch. The cross section of the phase shifter is shown in

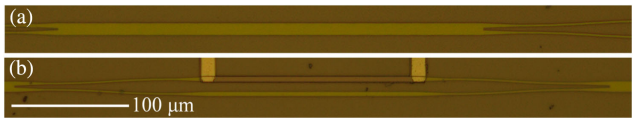

Fig. 3. Optical microscope images for (a) the MMI and (b) the phase shifter.

Fig. 1(a). A 200 μm long and 6 μm width Ti/W thin is placed 2 μm above the phase shifter. By increasing the width of the phase shifter, it remains mode insensitive even for higher-order modes (e.g., TE3 and TE4).

The device is fabricated using electron-beam lithography (EBL). The silicon device layer is patterned using a 100 keV EBL followed by an inductively coupled plasma-induced reactive ion etching process. The Ti/W thin film as metal heater and aluminum thin film for metal routing are deposited using electron beam evaporation. A thin (300 nm) SiO_2 passivation layer is deposited by chemical vapor deposition to protect the metal layers. The footprint of the mode insensitive switch is 1.1 mm × 12 μm. The optical microscope images of some key parts of the fabricated chip are shown in Fig. 3.

The continuous-wave (CW) test is done using a Keysight C-band tunable laser. The output of the laser source is connected to a polarization controller (PC), then coupled into the chip using a grating coupler. The output of the device is coupled out using another grating coupler. The optical output is measured using an ILX Lightwave optical power meter. All CW measurements are normalized to a loop back structure that connects two grating couplers with a short waveguide. The measured IL for the loop back structure is approximately −22 dB at 1550 nm.

Figure 4 shows the normalized output power as a function of the applied voltage to the phase shifter at 1560 nm. All three modes are fed into the upper input port of the MZI. When no voltage is applied to the phase shifter, all three modes propagate to the lower output port of the MZI. The mode insensitive switch works in its cross state. If proper voltage is applied, the phase in one arm for all three modes is changed by π. The switch is working in its bar state. The result shows that for TE0, the switch occurs at 2.46 V where the ER is approximately 34.5 dB. For TE1, 2.38 V is needed to realize switching where the ER is approximately 35.5 dB whereas, for TE2 mode, the switch voltage is 2.32 V, and the corresponding ER is approximately 23 dB. The switch voltage difference between these three modes is less than 0.14 V (±3%). The minor difference between the simulation results in Fig. 2(d), and experimental results can be attributed to the different phase response of the 3 dB splitter for three input modes. To trade-off the ER performance for the three modes, we set the switch voltage at 2.4 V in the all our following experiments. At 2.4 V, the switch still shows mode

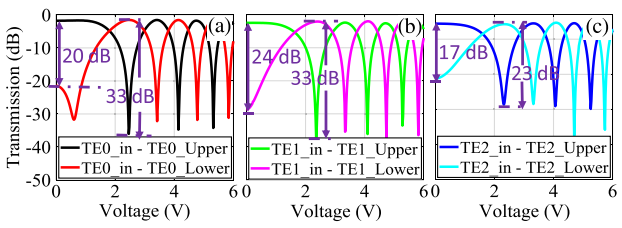

Fig. 4. Measured normalized transmission versus the applied voltage for (a) TE0 input, (b) TE1 input, and (c) TE2 input.

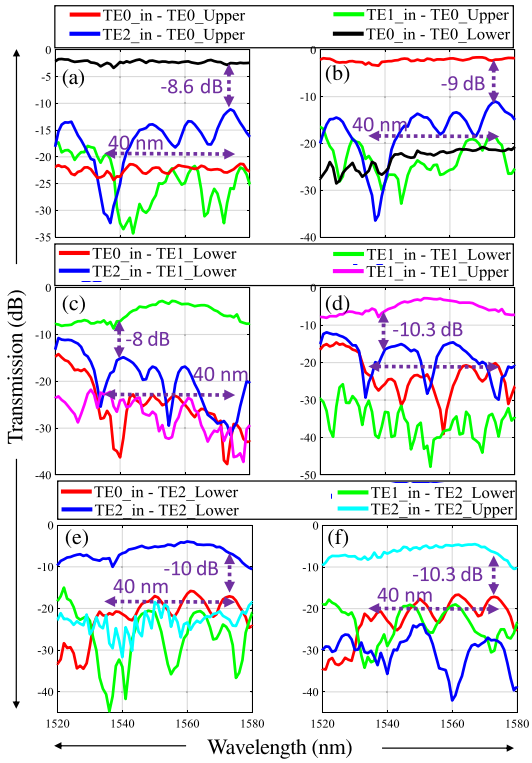

Fig. 5. Measured normalized transmission spectrum as a function of wavelength for (a) the cross state of TE0 input, (b) the bar state of TE0 input, (c) the cross state of TE1 input, (d) the bar state of TE1 input, (e) cross state of TE2 input, and (f) the bar state of TE2 input.

insensitivity. At this bias, the ER at 1560 nm for TE0, TE1, and TE2 is 20.7, 26.5, and 17.8 dB, respectively.

Figure 5 shows the corresponding spectrum response when the switch is working in its cross and bar states for the three different input modes. For TE0, TE1, and TE2 mode, the insertion loss (IL) is −2 (−2.1), −3.6 (−3.2), and −5.1 dB (−5.7 dB), respectively, for the cross (bar) state at 1550 nm. Half of the IL originates from the deMUX corresponding to approximately −1, −1.9, and −3.8 dB at 1550 nm for the TE0, TE1, and TE2, respectively. The crosstalk for TE0 is approximately < -8.6 dB and < -9 dB for the cross and bar states within the wavelength range from 1535–1575 nm. For TE1, the crosstalk is < -8 dB and < -10.3 dB for the cross and bar states within the same wavelength range. For TE2, the crosstalk is < -10 dB and < -10.3 dB for the cross and bar states within the same wavelength range. The detailed experimental results for the mode insensitive switch at 1550 nm are summarized in Table 1.

The payload transmission is conducted to demonstrate the switch performance in MDM data transmission systems. In this part, to show the impact of the crosstalk, we divide the experiment into two parts. In the first part, only one mode is transmitted while, in the second part, the three TE modes are transmitted simultaneously. Figure 6 shows the experimental setup of our data transmission system. The laser output is sent to a PC, then modulated by a 10 Gb/s NRZ PRBS31 electrical signal from the pulse pattern generator (PPG) using a modulator with 12.5 GHz 3 dB bandwidth. The modulated optical signal then goes through a 1 × 3 power splitter to generate

Table 1. Experimental Results of the Switch at 1550 nm

	Modes			
	TE0 (Cross/Bar)	TE1 (Cross/Bar)	TE2 (Cross/Bar)	Difference (Cross/Bar)
IL (dB)	−2.0/−2.1	−3.6/−3.2	−5.1/−5.7	3.1/3.6
ER (dB)	20.1/19.5	22.8/33.7	15.4/18.1	7.4/15.6
XT (dB)	−11.9/−11.5	−13.2/−13.9	11.9/−11.8	1.3/2.4
BW (nm)	40/40	40/40	40/40	0/0

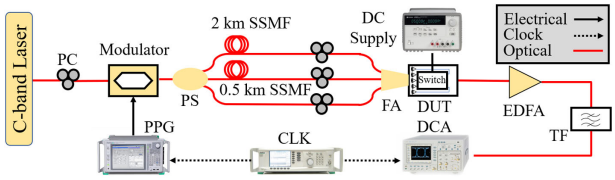

Fig. 6. Experimental setup for validation of the proposed mode insensitive switch. The black solid, black dotted, and red line represents electrical, clock, and optical signals, respectively. PC: polarization controller; PS: power splitter; SSMF: standard single-mode fiber; FA, fiber array; DUT, device under test; EDFA, erbium-doped fiber amplifier; TF, tunable filter; DCA, digital communication analyzer; PPG, pulse pattern generator.

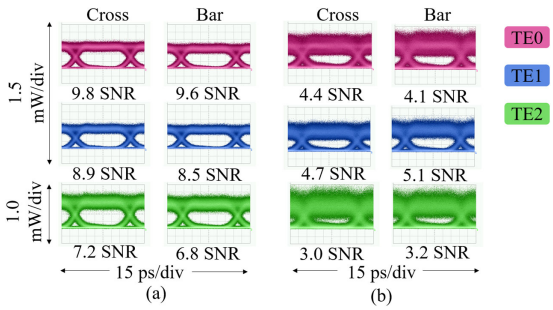

Fig. 7. Eye diagrams for (a) single-mode transmission and (b) three-mode transmission simultaneously.

three channel signals. One of the channels is delayed by passing through a 2 km standard single-mode fiber (SSMF), while the other channel is passing through a 0.5 km SSMF to decorrelate the three inputs. After that, another PC is used for each of the channels to ensure that only TE mode will be excited on the chip. Then the light is coupled into the device under test (DUT) using a grating coupler. The output from the DUT is amplified using an erbium-doped fiber amplifier (EDFA) to compensate for the excess loss of the setup. A C-band tunable c is employed to filter out the unwanted noise. Then the signal is sent to the digital-communication analyzer (DCA) with an integrated photodetector module to capture the eye diagrams.

The corresponding eye diagrams are also shown in Fig. 7. For signal mode transmission, clear eye diagrams are observed. However, for simultaneous transmission, the eye diagrams are deteriorated by the crosstalk from other modes. The TE2 mode channel suffers more from the deterioration, since the IL for TE2 is higher than that of the TE0 and TE1 channels. More importantly, from Fig. 5, one can find that the crosstalk from TE0 and TE1 almost has the same amplitude whereas, for the TE0 and TE1 channels, only one crosstalk from another channel dominates. Nevertheless, in all the scenarios, open eyes can be seen, and the performance can be improved by further optimizing the multimode 3 dB splitter which is the main source of the crosstalk. The crosstalk can be reduced using multiple input and multiple output digital signal processing techniques [17].

In conclusion, we propose and experimentally demonstrate a novel mode insensitive switch for MDM system. By sharing the phase shifter for different modes, the power consumption of the MDM switch is considerably reduced. The mode insensitive switch exhibits less than −8.6 (−9), −8 (−10.3), and −10 dB (−10.3 dB) within the wavelength range of 40 nm (1535–1575 nm) for the cross (bar) states for TE0, TE1, and TE2 modes, respectively. The ERs for the cross (bar) states are approximately 20.1 (19.5), 22.8 (33.7), and 15.4 dB (18.1 dB) for the TE0, TE1, and TE2 modes, respectively. Open eye diagrams from the data transmission for single and simultaneously three modes demonstrate the compatibility of the proposed switch with MDM data transmission systems. Further, the proposed switch structure is also scalable to even higher-order mode by further optimizing the 3 dB mode insensitive power splitter [3] and increasing the phase shifter width.

Funding. China Scholarship Council; Natural Sciences and Engineering Research Council of Canada.

Disclosures. The authors declare no conflicts of interest.

REFERENCES

1. E. Agrell, M. Karlsson, A. R. Chraplyvy, D. J. Richardson, P. M. Krummrich, P. Winzer, K. Roberts, J. K. Fischer, S. J. Savory, B. J. Eggleton, and M. Secondini, J. Opt. **18**, 063002 (2016).
2. C. Li, D. Liu, and D. Dai, Nanophotonics **8**, 227 (2018).
3. Y. Ding, J. Xu, F. Da Ros, B. Huang, H. Ou, and C. Peucheret, Opt. Express **21**, 10376 (2013).
4. H. Wu, C. Li, L. Song, H. K. Tsang, J. E. Bowers, and D. Dai, Laser Photonics Rev. **13**, 1800119 (2019).
5. X. Jiang, H. Wu, and D. Dai, Opt. Express **26**, 17680 (2018).
6. H. Xu and Y. Shi, Laser Photonics Rev. **12**, 1800094 (2018).
7. Y. Luo, Y. Yu, M. Ye, C. Sun, and X. Zhang, Sci. Rep. **6**, 23516 (2016).
8. X. Guan, Y. Ding, and L. H. Frandsen, Opt. Lett. **40**, 3893 (2015).
9. B. Stern, X. Zhu, C. P. Chen, L. D. Tzuang, J. Cardenas, K. Bergman, and M. Lipson, Optica **2**, 530 (2015).
10. M. Ye, Y. Yu, C. Sun, and X. Zhang, Opt. Express **24**, 528 (2016).
11. Y. Xiong, R. B. Priti, and O. Liboiron-Ladouceur, Optica **4**, 1098 (2017).
12. K. Chen, J. Yan, S. He, and L. Liu, Opt. Lett. **44**, 907 (2019).
13. H. Jia, S. Yang, T. Zhou, S. Shao, X. Fu, L. Zhang, and L. Yang, Nanophotonics **8**, 889 (2019).
14. R. B. Priti, G. Zhang, and O. Liboiron-Ladouceur, Opt. Express **27**, 14199 (2019).
15. R. B. Priti and O. Liboiron-Ladouceur, J. Lightwave Technol. **37**, 3851 (2019).
16. R. Halir, P. Cheben, J. M. Luque-González, J. D. Sarmiento-Merenguel, J. H. Schmid, G. Wangüemert-Pérez, D. Xu, S. Wang, A. Ortega-Moñux, and Í. Molina-Fernández, Laser Photonics Rev. **10**, 1039 (2016).
17. S. O. Arik, J. M. Kahn, and K.-P. Ho, IEEE Signal Process. Mag. **31**, 25 (2014).